HOKKAIDO UNIVERSITY

Title	Mode Coupling between Translation and Rotation in Repulsive Desorption
Author(s)	Matsushima, Tatsuo
Citation	e-Journal of Surface Science and Nanotechnology, 23(3), 213-221 https://doi.org/10.1380/ejssnt.2025-036
Issue Date	2025-06-21
Doc URL	https://hdl.handle.net/2115/95921
Rights(URL)	https://creativecommons.org/licenses/by/4.0/
Type	journal article
File Information	E-JSSNT2025 Pub Matsushima Mode Coupling review.pdf

Hokkaido University Collection of Scholarly and Academic Papers : HUSCAP

eJSSNT Review Paper

e-Journal of Surface Science and Nanotechnology **23**, 213–221 (2025)

Mode Coupling between Translation and Rotation in Repulsive Desorption

Tatsuo Matsushima †

Catalysis Research Center, Hokkaido University, North 21 West 10, Sapporo 001-0021, Japan
† *Corresponding author: tatmatsu@mbr.nifty.com*

Received: 3 March, 2025; Accepted: 14 May, 2025; J-STAGE Advance Publication: 21 June, 2025; Published: 21 June, 2025

In the repulsive desorption of hyperthermal products, rotation and translation are simultaneously excited by a common repulsion, resulting in mode coupling (MC). This review highlights the MC in repulsive desorption since it plays a key role in both the energy partitioning (EP) of the products to each mode and the structural sensitivity of desorption dynamics. It has long been overlooked due to non-angle-resolved (AR) energy analysis that ignores the desorption-angle dependence of the rotational and translational energies. The non-AR flux or energy analysis has prevented the desorption dynamics from being structure-sensitive since the structural information of desorption sites (symmetry, slope, and transition state orientation) can be extracted from the anisotropy of the product flux and energy distributions. Typical examples of the EP due to MC between translation and rotation include the combinative D_2 desorption on Cu(111), and the N_2 desorption from the decomposition of adsorbed N_2O on Pd(110)(1×1). For the former, the released energy is largely conserved in desorbed D_2 and the anti-correlation between the rotational and translational energies is clear. For the latter, the anti-correlation is weak due to the intense energy dissipation before desorption. An explanation is given for the misuse of the detailed balance principle in non-equilibrium desorption.

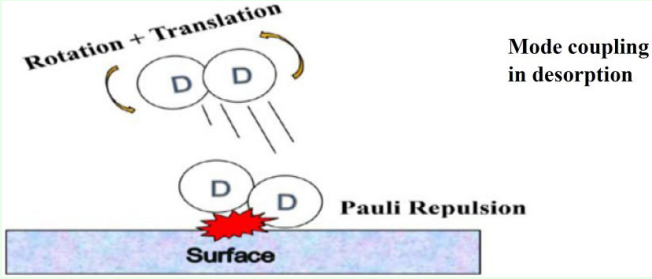

Keywords *Mode coupling; Energy partitioning; Desorption anisotropy; Desorption dynamics; Detailed balance principle*

I. INTRODUCTION

Through angle-resolved (AR) product desorption analysis, structure-sensitive desorption dynamics (SSDD) can provide structural information of the product emission site, such as symmetry, slope, and transition state (TS) orientation [1–3]. This is a unique method that obtains structural information of the surface active site directly from the reaction itself, as opposed to indirect information obtained from non-reacting objects, such as surface vibration spectroscopy and scanning microscopy. SSDD is based on the anisotropic distribution of the flux and energy of hyperthermal products. For further developments of SSDD, this review highlights the mode coupling (MC) between translation and rotation in repulsive desorption, since this coupling is induced by their simultaneous excitation due to a common repulsion [4–6] and plays an essential role in both the energy partitioning (EP) of the product into each mode and the structure sensitivity of desorption dynamics. This MC has long been overlooked in the current non-AR resonance-enhanced multiphoton ionization (REMPI) combined with time-of-flight (TOF) technique, which ignores the desorption-angle dependence of both rotational and translational energies, neglecting the desorption anisotropy [7, 8]. In this combination, state-selected product ions are collected by a single ion collector with a fixed acceptance angle in a time-resolved manner. In order to evaluate the EP due to the MC, the performance of AR-REMPI-TOF (state-selected ions are time-resolved and collected by a screen with imaging) is required to measure both energies in simultaneous, state-selective, and AR-TOF fashions since their energies are more or less anti-correlated, varying in opposite directions with an increasing desorption-angle shift from the collimation position.

Non-AR measurements of both energies were already reported for combinative D_2 (or H_2) desorption on Cu(111) [9, 10] and have recently been reported for N_2 released from the decomposition of N_2O(a) [(a) denotes an adsorption state] on Pd(110)(1×1) [11] by means of time-slice velocity-map

ion imaging (TSVMII) combined with REMPI. Although there are few reports that analyze both energies in simultaneous and AR fashions, this new report allows us for the first time to roughly compare the anti-correlations arising from two typical MCs. In this review, we discuss the limited confirmation of MC in repulsive desorption, since desorption of D_2 and N_2 exemplify quite different EPs [10, 11]. For the former D_2 on Cu(111), the anti-correlation between both energies is clear and will be quantitatively evaluated by the upcoming AR-REMPI-TOF, as shown in Section III. For the latter N_2 in the decomposition of N_2O(a), the anti-correlation is not easily confirmed due to large energy dissipation during the peculiar swing desorption of nascent N_2(a) [11, 12], as described in Sections IV and V.

The above confusion in repulsive desorption dynamics is also due to the misuse of the detailed balance principle (DBP) in non-equilibrium desorption, in addition to the oversight of MC in repulsive desorption. This misuse of DBP started with Willigen's desorption model [7, 8, 13]. Willigen misapplied DBP to non-equilibrium H_2 desorption when he found a sharp angular distribution of the flux of hydrogen desorbed on a metal surface and proposed that the acceleration of translational energy in desorption is due to repulsion caused by the activation energy barrier responsible for H_2 dissociative adsorption, i.e., the incidence angle dependence of H_2 dissociation (maximum dissociation at normal incidence) was replaced by the desorption angle dependence of hyperthermal molecules desorbing beyond the energy barrier within the DBP framework. This substitution of energy walls is the misuse of DBP since DBP comes from the second law of thermodynamics and is therefore only valid at equilibrium. The balance is on the forward and reverse reaction rates (and energy flow) on each elementary step, not on the height of the energy wall that governs the reaction rate [2].

Auerbach *et al.* extended the Willigen model to each energy mode when they succeeded in simultaneously measuring the vibrational, rotational, and translational energies of D_2 produced on Cu(111) using the non-AR-REMPI-TOF [9]. They found the anti-correlation between the rotational and translational energies in each vibrational state of D_2 at j (rotational quantum number) > 6. This anti-correlation was explained by the energy required for dissociation of the incident D_2 within the DBP framework, by referring to their results of D_2 dissociation on Cu(111) by means of seeded molecular beams. That is, when the vibration is excited, the energy required for dissociation decreases accordingly, and the remaining energy is overcome by the cooperation of the translational and rotational energies, leading to dissociation. The required translational energy is smaller in high rotational energy states. Each observed energy in desorption was separately used to simulate the dissociation rate to justify the use of DBP in desorption dynamics. Thus, the energy distribution of desorbed D_2 has long been explained based on the adsorption dynamics, and the MC in repulsive desorption was overlooked. This scheme was certainly driven by the translational energy maximum around j = 5 (which disappeared as an error in the reanalysis 21 years later [10]). It takes more time to revise the energy flow in repulsive D_2 desorption since quantitative confirmation of the EP requires the future AR-REMPI-TOF. More details are summarized in Section VII.

II. ENERGY PARTITIONING IN REPULSIVE DESORPTION

With the development of picosecond lasers, the vibrational energy relaxation of ad-molecules on metal surfaces was confirmed on the order of picoseconds in the 1990s [14]. Before the energy relaxation, for example, CO(a) on Pt(111) can vibrate more than 100 times [15]. Molecules combinatively formed on the surface are likely to be vibrationally excited by the release of bond energy immediately after formation, so the resultant product may react or desorb before relaxing. In fact, hyperthermal products are often found in combinative desorption or associated with combinative processes [3, 8]. The concept of EP into each mode is indispensable in product desorption dynamics dealing with the flow of energy [4].

The EP into translational and rotational modes is well known in the decomposition of triatomic molecules in the gas phase since Pauli repulsion is induced between the bonded atoms during decomposition, and the released energy is stored in the products [16]. The resulting repulsive force excites both rotation and translation of the molecular product. Here, the anti-correlation is found between the rotational and translational energies of the product. Similar EP occurs for the translation and rotation of hyperthermal products in repulsive desorption on metal surfaces. Such repulsive desorption takes place when a nascent product is born on a repulsive part of the potential energy surface; for example, a bulky product is formed near the surface. The resultant repulsive force is originated from the Pauli repulsion as seen at the bond rupture. It excites not only the torque leading to the rotation of the product but also the translation (Figure 1). Their modes are coupled with each other since those are excited by a common repulsion [5, 6]. As this desorption is completed much faster (about 100 fs [17]) than the relaxation of vibrationally excited ad-molecules, anti-correlation is likely between both energies even if some energy leaks into

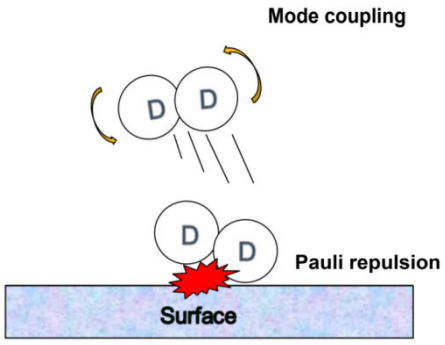

Figure 1: Repulsive and combinative desorption excites both rotation and translation by a common repulsion, as sketched for 2D(a) → D_2(g) [(g) denotes a gaseous state].

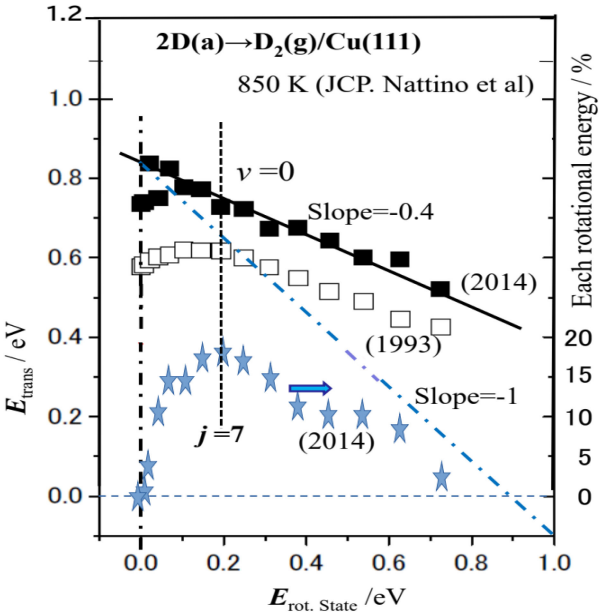

Figure 2: Observed translational and derived rotational energies of D_2 on Cu(111) vs. the energy of rotational states. EP largely shifts to translation. Energy is supplied by vibrational transitions [1]. □: Old translational energy in 1993 [9]. ■: Reanalyzed translational energy in 2014 [10]. ★: Derived rotational energy at each j (%).

other modes. Other energy dissipations, such as chemi-currents and electron-hole pair excitation, are minor [18, 19].

In fact, the anti-correlation has already been noticed between rotational and translational energies in the combinative desorption of D_2 on Cu(111) (see Figure 2); unfortunately, the results have long been explained by adsorption dynamics, invoking the DBP as mentioned above [7–10]. The anti-correlation between both energies is useful for SSDD. However, due to the lack of AR-REMPI-TOF, the EP into translational and rotational modes on metal surfaces has not yet been quantitatively evaluated. To evaluate this EP, the anti-correlation between both energies needs to be examined from their desorption-angle dependence. In order to establish the standard anti-correlation in repulsive desorption, some suitable model systems with the following characteristics should be selected: (i) The energy released in each desorption is nearly constant. (ii) AR-REMPI-TOF analysis is possible for hyperthermal products to evaluate both translational and rotational energies simultaneously. Of course, the EP takes place in repulsive desorption even if the energy dissipation is significant.

The combinative desorption of H_2 (or D_2) on Cu(111) is one of the suitable model systems since it shows an isotropic flux distribution around the normally directed axis [20] and is likely to be close to an elastic collision (no energy loss) due to the large mass ratio of m_{Cu}/m_{H2} where m is the atomic or molecular weight. On the other hand, N_2 desorption from N_2O(a) decomposition on Pd(110)(1×1) is expected to significantly lose energy before desorption. This is because it proceeds through the peculiar swing motion relatively slowly as compared with electronic structure changes due to desorption [11, 12] and the mass ratio of m_{Pd}/m_{N2} is much smaller than that of m_{Cu}/m_{H2}. These facts may increase the inelastic effects, making it hard to clearly see the anti-correlation, as detailed in Sections IV and V. Non-AR-REMPI-TOF data from other desorption systems such as H_2 on Ni(111) [21] and Ag(111) [22] and N_2 on Cu(111) [23] and Ru(0001) [24], cannot be used for comparison with the anti-correlation due to insufficient data, as described in more detail in Section VI [8].

The general trend of the anti-correlative energy change of the EP is already seen for the product CO_2 in CO oxidation on Pd(111), where the rotational temperature increases with increasing desorption angles [25]. Such angular dependence of the rotational temperature was examined with AR infrared emission analysis only for product CO_2 in CO oxidation on Pd(111) and Pd(110). However, it is not a state-selective measurement, since CO_2 is not state-selectively ionized by REMPI. The decrease in translational energy at large desorption angles is more or less observed for hyperthermal products such as CO_2, N_2, and H_2 (or D_2) on metal surfaces [26, 27].

III. ENERGY PARTITIONING IN D_2 DESORPTION

Prior to the REMPI work of desorbed H_2 [28], the EP due to the coupling of rotational and translational modes of hyperthermal products received little attention in desorption dynamics since their energies were separately analyzed in non-state-selective or non-AR manners [25–27, 29, 30]. Even after the non-AR-REMPI-TOF work of H_2 (or D_2) desorption on Cu(111) [7–9], the observed energies have been separately explained by adsorption dynamics within the DBP framework, as described in the introduction and detailed in Section VII. To examine the EP in repulsive desorption, it is important to simultaneously evaluate both energies in an AR fashion. Actually, the energy carried by the product molecules in repulsive desorption is not constant, due to the energy loss before desorption and dissipation due to inelastic collisions in the final desorption. In practice, two extreme cases of EP are recognized in repulsive desorption.

For the combinative desorption of D_2 (or H_2) on Cu(111), the anti-correlation is already noticed between the rotational and translational energies (Figure 2) [7, 10]. The plots were created by reading the quantities from Figures 9 and 13 in Ref. 10 and Figure 7 in Ref. 9. The derived rotational energies are expressed as a percentage of the total rotational energy. The rotational energy released is greatest around $j = 7$ and decreases rapidly with increasing j values as the number of high rotational energy D_2 decreases. In this non-AR-REMPI-TOF work, the sum of the translational energy (E_{trans}) and rotational state energy at each j ($E_{rot.state}$) increases linearly with increasing rotational state energy. This increase in the energy sum is largely due to an overestimation of the translational energy as ions of fixed rotational states are analyzed in the TOF format. It is caused by shortcomings in the experimental setup, as reported elsewhere [2]. Non-

AR-REMPI-TOF leads to an overestimation of the translational energy of high rotational energy states due to ignoring the signals at large off-normal angles, i.e., only ions within a fixed acceptance angle near the normal axis are collected by the ion collector, although the spatial distribution becomes broader with an increasing j value. The true energy sum is close to the energy value for $j = 0$. This D_2 desorption seems to be close to the limiting case of the EP where the energy released in repulsive desorption is nearly constant. To confirm this simple case, both the rotational and translational energies need to be examined by AR and state-resolved TOF analysis. However, such an analysis of both energies has not yet been performed. This is the main reason why the concept of MC has not yet been established in repulsive desorption. The blue dash-dotted line with a slope of −1 (Figure 2) shows the ideal case where D_2 desorbs without energy loss. The actual relationship should lie between this line and the observed line.

The dynamics of combinative desorption of hydrogen from Cu(111) has long been explained in terms of adsorption dynamics within the framework of DBP, where the EP step in the desorption pathway is omitted. In opposition to the use of DBP in desorption dynamics, and with reference to the translational energy observed at $j = 0$, we have proposed a new partitioning of the released energy due to the vibrational transitions of the nascent D_2(a) to lower energy levels into rotational and translational modes [1]. Comparing the amount of released energy with the vibrational energy of nascent D_2(a), the vibrational levels in a narrow energy range above v (vibrational quantum number) = 3 are likely to transition to lower energy levels. Such nascent D_2(a) states have not yet been predicted in theory.

IV. ENERGY PARTITIONING IN N_2 SWING DESORPTION

The repulsive desorption of product N_2 in the decomposition of N_2O(a) on Pd(110)(1×1) is another extreme example of EP, where the rotational and translational energies are weakly anti-correlated. This decomposition proceeds with a peculiar swing desorption of the nascent product N_2 [11, 12]. The energy dissipation before and during desorption is intense, and the residual energies just before the final desorption appear to be different. If the energy of the nascent $*N_2$(a) (* denotes a nascent state) just before desorption is dispersed, the anti-correlation cannot be easily confirmed.

This N_2 desorption takes place in the decomposition of [001]-oriented N–N–O(a) with small N_2O(a) coverage [31], and the product $*N_2$(a) is bi-directionally emitted along the [001] direction (Figure 3) [32]. It was first found in temperature-programmed desorption (TPD) of N_2O-covered Pd(110). Four N_2 desorption peaks appear in the range of 110–140 K, and three of them show similar bi-directional collimation. The sharp distribution of product N_2 is collimated around ±50°–±43° off-normal in an approximate $\cos^{28-50}(\theta \pm 47)$ form on the normally directed plane along the [001] direction, where θ is the desorption (polar) angle.

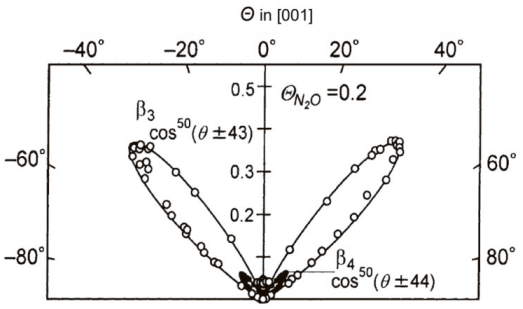

Figure 3: Desorption angle dependence of the desorbed β_3-N_2 peak on the (001) plane during TPD of N_2O-covered Pd(110). β_3-N_2 peaks at 123 K and β_4-N_2 at 110 K. Θ_{N2O}; N_2O coverage. The figure is a reproduction of Figure 3(b) in Ref. 32 [H. Horino *et al.*, Chem. Phys. Lett. **341**, 419 (2001)]. Copyright (2001) by Elsevier Science B.V.

The distribution becomes somewhat broader with higher coverage, and the collimation shifts to smaller off-normal angles. This off-normal desorption is insensitive to surface temperatures above 800 K in the steady state $N_2O + CO$ (or H_2) reaction [3].

Similar bi-directional N_2 emission along the [001] direction has also been observed on Rh(110)(1×1) [33] and Ir(110)(1×1) [34]. The collimation angle depends on the kind of metal and the coverage of N_2O(a). The collimation angle with low N_2O(a) coverage is approximately ±65° on Ir(110)(1×1) and ±70° on Rh(110)(1×1), and it is insensitive to the surface temperature. Furthermore, on Rh(100), four-directional N_2 desorption is directed at approximately 70° off-normal at low N_2O(a) coverage [35]. N_2O(a) decomposes to hyperthermal N_2(g) and O(a) on these surfaces even below the desorption temperature of N_2(a) [36]. The energetic product N_2 is released without being trapped on the surface.

From the density functional theory (DFT) with generalized gradient approximation (GGA) calculations of the potential energy surface of $*N_2$(a) on Pd(110), a swing desorption model was first proposed by Kokalj in 2002 [37], elaborated in 2015 [12], and reproduced by Wodtke's group in 2023 [11]. This is indeed a peculiar desorption pathway, as drawn in Figure 4. N_2O is a linear molecule, and on Pd(110), it is bent (180° → 156°) due to the charge transfer from the metal [Figure 4(i)]. It decomposes at surface temperatures of 90–165 K in TPD procedures [32, 38]. This wide range in the decomposition temperature is due to the adsorption (or activation) energy enhanced by deposited oxygen [3, 39]. The $*N_2$(a) swings to the opposite side on the adsorbed Pd atom immediately after the NN–O bond is broken [Figure 4(ii)]. The swing motion of the fragment $*N_2$(a) is caused by the Pauli repulsion between the bonded atoms, and the repulsive force should act totally from the counter product *O(a) toward the center of mass of desorbing $*N_2$(a) at the moment of N_2 detachment. The detachment can occur around the tilt angle of $*N_2$(a) at which the kinetic energy of the nascent $*N_2$(a) exceeds the adsorption bond energy. In the DFT-GGA calculations, the perpendicular form of N_2(a) is stable [Figure 4(iii)], and the bond energy decreases with increasing tilt

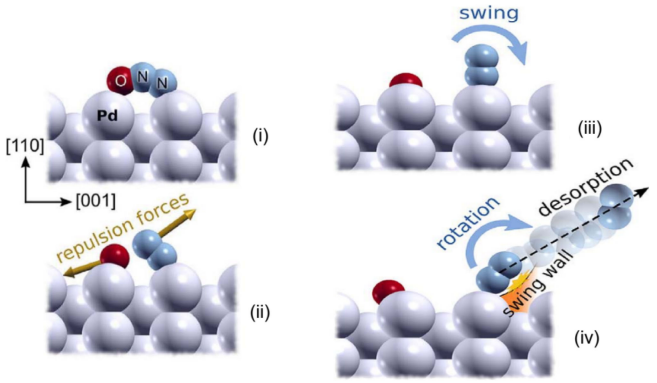

Figure 4: Typical snapshots of swing N_2 desorption during N_2O(a) decomposition on Pd(110)(1×1), sequentially from (i) to (iv) [12].

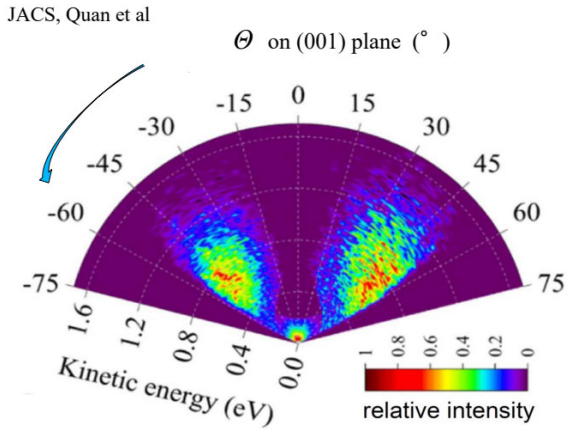

Figure 5: Velocity-selected N_2 ion images at $j = 10$ for the catalytic $N_2O + CO$ reaction on Pd(110) at 470 K. This figure is a reproduction of Figure 2(b) in Ref. 11 [J. Quan *et al.*, J. Am. Chem. Soc. **145**, 12044 (2023)] under CC-BY 4.0 license.

from the standing state; therefore, the scission of the bond is predicted at a tilt of about 45° on that opposite side [Figure 4(iv)] [12]. The final bond rupture between the $*N_2$(a) and the Pd atom is delayed by the swing motion after the first bond rupture between the terminal oxygen atom and the central nitrogen atom of PdNN–OPd.

This swing desorption proceeds during bridge-site adsorption [12]. The on-top site provides more stable adsorption for N_2O; however, the swing at this site does not allow N_2 to desorb and transition to a stable state parallel to the surface. The decomposition on top requires more energy for the movement of the counter product oxygen atom to be stabilized. The total activation energy for diffusion to the bridge site and decomposition there is more likely than that for the on-site adsorption of N_2O(a).

This swing motion at the bridge site is affected by the final repulsion from the swing wall of the bridge site [Figure 4(iv)]. Without this wall, the $*N_2$(a) would be stabilized into a lying form before desorption. This swing desorption scenario has been reproduced by molecular dynamic simulations in the above Göttingen group [11]. The energy source is mainly due to the heat of adsorption of the counter product O(a) (around 4.5 eV). This is consistent with the REMPI work that shows the absence of vibrationally excited N_2 in the product [11]. Since swing desorption involving a large nuclear motion is much slower than simple repulsive desorption, such as D_2 combinative desorption on Cu(111) as well as the change in electronic structures due to desorption, the released energy is likely to be dissipated significantly into the underlying metal lattice.

The EP into rotational and translational modes proceeds at the moment it leaves the surface, yielding the anti-correlation between both energies when the desorbing product has only a negligible amount of kinetic energy just before desorption, as seen in D_2 desorption. On the other hand, in the swing desorption mentioned above, the nascent N_2(a) is still likely to retain kinetic energy just before desorption. Furthermore, each final product retains high kinetic energy as expected from the sharp spatial distribution [11, 40]. In this case, the anti-correlation is not easily confirmed, even in TSVMII-REMPI work, as described in Section V.

V. ENERGY DISSIPATION IN N_2 SWING DESORPTION

Experimental confirmation of the swing desorption model requires evaluation of the strengths of the excited states of both rotation and translation of desorbed N_2 in an AR fashion because this hyperthermal product is off-normally emitted along the [001] direction. Recently, the combination of TSVMII with REMPI was used to evaluate the energy of each mode of product N_2 in the quasi-steady-state (pulsed beams of different reactants are separately dosed) catalyzed reaction of $N_2O + CO \rightarrow N_2 + CO_2$ on Pd(110)(1×1) at surface temperatures from 450 to 650 K [11]. This combination provides performance beyond AR-REMPI-TOF and confirmed the preceding conclusions and speculations (bi-directional desorption, excited rotation and translation [12]) of the swing desorption, except for the anti-correlation between rotational and translational energies.

In that report, two off-normal desorption of product N_2 with high translational energy at $j = 10$ are collimated around ±45° along the [001] direction (Figure 5). The maximum translational energy is seen around that collimation angle. The observed rotational states are widely distributed at energies much higher than those expected at the surface temperature. They are widely distributed over $j = 4$–53. The maximum population of the rotational energy state appears at $j = 16$–24. However, no desorption-angle dependence of the population of each rotational state is shown, although the data should be available. The spatial distribution from the ion images is broader than that in the previous results (Figure 3) [32], which is likely due to the variation of the surface N_2O coverage in the pulsed molecular beams. Unfortunately, this paper does not pay attention to the dependence of either translational or rotational energy on the desorption angle, nor does it discuss their physical meanings.

To investigate the dependence of the rotational energy (or rotational temperature) on the angle shift from the collima-

tion position, one has to examine the population distribution of each rotational energy state at different angles. The population distribution of each rotational state should depend on the desorption-angle shift. The velocity distribution of the AR rotational state extracted at each angle can provide the translational energy, which can be correlated to the rotational energy. The resultant rotational temperature can be correlated with the averaged translational energy over the rotational states.

Without population data for each rotational energy state, the rotational temperature (actual rotational energy) cannot be estimated. From the viewpoint of the MC, the rotational energy is expected to increase with an increasing shift from the collimation angle since the translational energy at a fixed rotational energy state decreases as seen in Figure 5 [11]. No direct comparison is possible between the translational and rotational energy at various desorption angles. Instead, the average (non-AR) translational energy of each rotational state slightly decreases (0.6 → 0.5 eV) with increasing rotational state energy (0 → 0.6 eV, $j < 48$). This kinetic energy value is consistent with the old value of 0.6 eV reported in non-state-selected TOF work using a mechanical chopper (in 1999) [40].

Without the desorption-angle dependence of the rotational energy, the result that the average translational energy slightly decreases with an increasing shift of the rotational energy state could be misread as indicating that there is no anti-correlation between translational and rotational energies. This weak anti-correlation could be somewhat improved to be more remarkable when the angle dependences of both energies are analyzed simultaneously. This is because non-AR translational energy is overestimated at high rotational energy states when product ions are partially collected around the collimation position. Such an overestimation was already experienced for the translational energy of the combinative D_2 desorption on Cu(111) [1, 2]. There, the kinetic energy is overestimated in the high rotational energy states, making the observed anti-correlation less sharp as the real correlation. This overestimation is due to the shortcomings of the non-AR type of REMPI-TOF, in that the fraction of ion collection decreases with increasing rotational energy.

In this bi-directional desorption analysis [11], the ions ejected at desorption angles above +60° (or below −60°) are ignored (Figure 5). With an acceptance angle of ±60°, this ion collection system ignores signals above 15° outward from the collimation axis (at ±45°), as seen by the asymmetric signal distributions around the collimation axis. This asymmetric collection of signals on the normally directed plane along the [001] direction affects the estimation of the averaged translational energy. Ignoring signals at such large angle shifts from the collimation axis will result in an overestimation of the averaged (non-AR) translational energy. The actual anti-correlation should be more pronounced. Fortunately, the trace of the anti-correlation in repulsive desorption is still noticeable. This correlation must be evaluated by means of the energy analysis of each mode of desorbed product in state-selective and AR fashions.

VI. ENERGY DISSIPATION AND DESORPTION DYNAMICS

The proposed swing desorption scheme consists of at least five energy transfer steps. (i) The first repulsion occurs between nascent N_2(a) and the counter product O(a), inducing a large amount of kinetic (torque) energy into the nascent N_2(a) and partially dissipating it in the diffusion of the product O(a). (ii) During the following swing motion, the kinetic energy is dissipated into the underlying metal lattice. (iii) The nascent N_2(a) is desorbed at a tilt angle of about 45°, where the swing kinetic energy exceeds the adsorption energy, which decreases with tilt beyond the stable vertical. (iv) Repulsion acts between the nascent N_2(a) and the Pd atoms, releasing rotationally and translationally excited N_2. (v) The final repulsion acts from the swing wall consisting of the surface Pd atoms.

In this N_2 desorption, we have no information about either the energy transfer during the swing motion or the energy state of the nascent N_2(a) immediately before desorption. No clear anti-correlation is expected between rotational and translational energies since many energy-loss processes before the final desorption lead to various energy states of nascent N_2(a) just before desorption. Nevertheless, the [001] orientation of TS is still preserved in the spatial distribution of the product N_2 and its translational energy distribution, and repulsive product release still proceeds. Here we see the inherent difficulty in establishing product desorption dynamics in surface reactions. Only the final desorption process before relaxation, regardless of the position of a rate-determining step, can be studied at the dynamic level, while surface processes before desorption have been studied little at the dynamic level due to the difficulty of energy analysis of nascent products on the surface.

Even if the heat of reaction is large (or the dissociative adsorption is highly activated), the resultant product is not always repulsively desorbed. An energetic product is easily thermalized before desorption when the molecule is once trapped on the surface after formation. The relaxation time of vibrationally excited ad-molecules on a metal surface is much shorter than the surface residence time of ad-molecules [14]. The latter residence is in the order of nanoseconds or longer even in physical adsorption around 500 K [2]. Hodgson's group used atomic beams or thermal decomposition of NH_3 to prepare N-covered noble metal surfaces and studied the combinative desorption of N_2 by means of non-AR-REMPI-TOF under TPD or pulsed atomic beams conditions [41]. The bond energy of N–N (9.76 eV) is large, but in the case of 2N(a) → N_2(a) desorption, the translational and rotational modes of the desorbed N_2 are already in equilibrium with the surface temperature on Pd(110) and Pt(100) [8, 41]. Strong repulsive desorption is seen on nascent N_2 on Cu(111). The angular distribution is sharp in a $\cos^{28}\theta$ form, the translational energy is large 4.2 eV at $v = 0$ and 4.0 eV at $v = 1$, and the rotational temperature is 900 K (0.077 eV) at a surface temperature of 700 K, which is less than 2% of the translational one. The vibrational temperature is 5100 K.

These results are mostly due to the N_2 desorbed along the surface normal because of the sharp angular distribution, suggesting a TS parallel to the surface plane. However, no anti-correlation is confirmed between rotational and translational energies since no angle dependence of either energies is given. On the other hand, the results on Ru(0001) fall between the above two cases. The averaged translational energy is 0.42 eV at $v = 0$ and 0.40 eV at $v = 1$; therefore, the repulsion is not weak, and the translational energy is widely distributed. The population is highest around the translational energy of 0.05 eV and, spreading out to about 2 eV. Different repulsive forces or various EPs seem operative, suggesting interesting MCs when AR-REMPI-TOF could be available.

There are two main reasons the development of desorption dynamics on surfaces has long been delayed. First, the angle dependence of the rotational energy has been overlooked and still has not been observed. Second, there has been long-standing misuse of DBP in desorption dynamics. More than half a century has passed since the first report of non-equilibrium product desorption, which contradicts the basic assumption of surface chemical reaction kinetics. To describe surface reactions, it is urgent to combine at least both chemical reaction kinetics and desorption dynamics. The former deals with the reaction rate, whereas the latter deals with the flow of energy.

VII. CONFUSED DYNAMICS OF REPULSIVE DESORPTION

This section clarifies the root cause of the confusion in repulsive desorption dynamics. As described in the introduction, the direct causes are (i) overlooking rotational and translational MC in repulsive desorption, and (ii) misuse of DBP in non-equilibrium desorption. Both of these problems are caused by the fact that the desorption angle dependence of translational and rotational energies is not taken into account in non-AR-REMPI-TOF measurements. Although the angle dependence of translational energy in repulsive desorption was well known in the 1970s, this contradiction was not corrected for a long time. In this section, we examine the development of hydrogen desorption dynamics, which has been the stage for cutting-edge measurements in repulsive desorption dynamics. Herein lies the difficulty of AR-REMPI-TOF, which is required for the next stage of SSDD.

The concept of EP in repulsive desorption is reminiscent of the old discussion started from the non-state-selective TOF work dating back to the 1970s [26, 42]. Observations show that the translational temperature of H_2 combinatively desorbed along the surface normal on Ni(111) is higher than the surface temperature, decreases with increasing desorption angles, and becomes lower than the surface temperature for desorption angles above 60°. Meanwhile, similar decreases in translational energy at high desorption angles have frequently been observed for repulsive product desorption. However, the decreasing mechanism of the translational energy has never been adequately explained [41]. Those decreases can be explained now by the EP for rotational and translational modes.

The lack of a proper explanation seems due to the absence of both the observed desorption angle dependence of the rotational energy and the concept of the MC in repulsive desorption. These have long been concealed by the inappropriate use of DBP in desorption dynamics. The desorption-angle dependence of rotational energy has not yet been examined for hyperthermal desorption except for AR (non-state selective) rotational temperature analysis of infrared emission from nascent CO_2 in the oxidation of CO on palladium [25].

The use of DBP in desorption dynamics is based on the assumption that the dynamics of adsorption and desorption are invariant even far from equilibrium, i.e., the distributions of the product fluxes and translational, rotational and vibrational energies are invariant across the conditions of adsorption and desorption measurements. This assumption is invalid because those distributions are sensitive to experimental conditions in many hyperthermal desorption systems, especially to the reactant coverage [3] except for H_2 (or D_2) desorption on Cu surfaces. The reason DBP has been used incorrectly for a long time is the impossibility of investigating the desorption dynamics depending on the coverage of surface hydrogen on copper surfaces at high temperatures. The dynamics of both adsorption and desorption of H_2 (or D_2) on Cu(111) have been most thoroughly investigated with DBP, and the results have justified its use in desorption dynamics [43]. In fact, the best hydrogen source for desorption dynamics work is the permeation of atoms through a sample crystal. The stable desorption flux and reduced background signals allow high-quality data to be obtained. The resultant dynamic parameters estimated from the distributions of translational, rotational, and vibrational energies are so beautiful that the atomic (or molecular) beams work following these results has not overcome the preceding work, especially at low j values [8]. This permeation can be used only at high temperatures, for example, above 750 K on Cu surfaces and cannot change the amount of surface hydrogen (almost zero coverage).

Furthermore, the translational energy of desorbed D_2 showed a maximum value around $j = 6$ as the rotational energy increases (Figure 2) as mentioned in Section I [9]. This was explained in the framework of the DBP as the steric effect of the incident molecule on adsorption. This explanation had long supported the use of DBP in repulsive desorption dynamics. However, that maximum disappeared as experimental errors in the re-analyzed results 21 years after the first report [11]. Instead, the EP model of rotational and translational modes can well explain the revised linear relation (without the maximum) between both energies [2].

EP into rotation and translation is mainly controlled by the tilt of the TS and the magnitude of the repulsive force from the surface. If the TS toward product H_2 is parallel to the surface plane, the energy is mainly partitioned into translational modes since it is difficult to excite rotational torques. On the other hand, when the TS is tilted with respect to the

site plane, the torque motion can be easily excited by the repulsive force exerted by the surface. If the EP is significantly shifted to the rotational mode, the translational temperature can be even lower than the surface temperature. Such an explanation will be justified by simultaneously examining both the translational and rotational energies by AR-REMPI-TOF.

What prevents the improvement of non-AR-REMPI-TOF to AR-REMPI-TOF is the extreme signal drop. When using a collimator in the AR procedures, the drop is two to three orders of magnitude (depending on the angular resolution) [44, 45]. This drop can be avoided to some extent by performing time-resolved imaging (no ion loss, short flight paths) of ions from REMPI [11]. However, this requires a hemispherical field-free space that does not perturb the trajectories of ions with energies below 0.5 eV. The fact that distortions are also seen in the imaging of N_2 ions (Figure 5) suggests difficulties with the lighter H_2 ion. These appear to be the final technical hurdles. Once AR-REMPI-TOF is realized, it will be possible to quantitatively evaluate the EP by MC and to validate theoretically calculated potential energy surfaces by using structural information of surface active sites (composed of multiple surface atoms [2]) obtained from SSDD.

VIII. SUMMARY

MC between rotation and translation in repulsive desorption improves the desorption dynamics of hyperthermal products. For further developments of SSDD, the following points should be changed or performed:

(i) Non-AR-REMPI-TOF should be changed to AR-REMPI-TOF to examine the concept of MC.
(ii) Quantitative confirmation of EP should be performed in H_2 and D_2 desorption on copper surfaces to establish the standard MC in repulsive desorption.
(iii) The concept of MC is useful for SSDD because the energy anti-correlation between rotational and translational modes can predict dynamics changes in either one.

Acknowledgments

This work was partly supported by a 1996 grant from the Center of Excellence Special Equipment Program of the Ministry of Education, Sports, and Culture of Japan and by Grant-in-Aid No. 21550004 for General Scientific Research from the Japan Society for the Promotion of Science (JSPS).

References

[1] T. Matsushima, e-J. Surf. Sci. Nanotechnol. **22**, 188 (2024).
[2] T. Matsushima and A. Kokalj, Surf. Sci. Rep. **73**, 191 (2018).
[3] T. Matsushima, Prog. Surf. Sci. **82**, 435 (2007).
[4] T. Matsushima and K. Shobatake, J. Mol. Cat. A **315**, 135 (2010).
[5] K. Yang and T. S. Rahman, J. Chem. Phys. **93**, 6834 (1990).
[6] T. Brunner and W. Brenig, Surf. Sci. **317**, 303 (1994).
[7] C. T. Rettner, D. J. Auerbach, J. C. Tully, and A. W. Kleyn, J. Phys. Chem. **100**, 13021 (1996).
[8] A. Hodgson, in: *The Chemical Physics of Solid Surfaces*, Vol. 11, edited by D. P. Woodruff (Elsevier, Amsterdam, 2003) p. 143.
[9] H. A. Michelsen, C. T. Rettner, D. J. Auerbach, and R. N. Zare, J. Chem. Phys. **98**, 8294 (1993).
[10] F. Nattino, A. Genova, M. Guijt, A. S. Muzas, C. Díaz, D. J. Auerbach, and G.-J. Kroes, J. Chem. Phys. **141**, 124705 (2014).
[11] J. Quan, R. Yin, Z. Zhao, X. Yang, A. Kandratsenka, D. J. Auerbach, A. M. Wodtke, H. Guo, and G. B. Park, J. Am. Chem. Soc. **145**, 12044 (2023).
[12] T. Matsushima and A. Kokalj, J. Phys. Chem. C **119**, 11699 (2015).
[13] W. Van Willigen, Phys. Lett. A **28**, 80 (1968).
[14] H. Ueba, Prog. Surf. Sci. **55**, 115 (1997).
[15] R. R. Cavanagh, E. J. Heilweil, and J. C. Stephenson, Surf. Sci. **283**, 226 (1993).
[16] J. C. Polanyi, Acc. Chem. Res. **5**, 161 (1972).
[17] H. Arnolds and M. Bonn, Surf. Sci. Rep. **65**, 45 (2010).
[18] E. Hasselbrink, Curr. Opin. Solid State Mater. Sci. **10**, 192 (2006).
[19] X. Luo, B. Jiang, J. I. Juaristi, M. Alducin, and H. Guo, J. Chem. Phys. **145**, 044704 (2016).
[20] M. Balooch and R. E. Stickney, Surf. Sci. **44**, 310 (1974).
[21] S. Wright, J. F. Skelly, and A. Hodgson, Faraday Discuss. **117**, 133 (2000).
[22] F. Healey, R. N. Carter, G. Worthy, and A. Hodgson, Chem. Phys. Lett. **243**, 133 (1995).
[23] M. J. Murphy, J. F. Skelly, and A. Hodgson, J. Chem. Phys. **109**, 3619 (1998).
[24] M. J. Murphy, J. F. Skelly, A. Hodgson, and B. Hammer, J. Chem. Phys. **110**, 6954 (1999).
[25] T. Yamanaka and T. Matsushima, Phys. Rev. Lett. **100**, 026104 (2008).
[26] G. Comsa and R. David, Surf. Sci. Rep. **5**, 145 (1985).
[27] T. Matsushima, Surf. Sci. Rep. **52**, 1 (2003).
[28] G. D. Kubiak, G. O. Sitz, and R. N. Zare, J. Chem. Phys. **81**, 6397 (1984).
[29] K. Kunimori and G. L. Haller, Bull. Chem. Soc. Jpn. **65**, 2450 (1992).
[30] H. Uetsuka, K. Watanabe, and K. Kunimori, Surf. Sci. **363**, 73 (1996).
[31] K. Watanabe, A. Kokalj, Y. Inokuchi, I. Rzeznicka, K. Ohshimo, N. Nishi, and T. Matsushima, Chem. Phys. Lett. **406**, 474 (2005).
[32] H. Horino, S. Liu, A. Hiratsuka, Y. Ohno, and T. Matsushima, Chem. Phys. Lett. **341**, 419 (2001).
[33] H. Horino, I. Rzeźnicka, A. Kokalj, I. Kobal, Y. Ohno, A. Hiratsuka, and T. Matsushima, J. Vac. Sci. Technol. A **20**, 1592 (2002).
[34] T. Matsushima and A. Kokalj, Appl. Surf. Sci. **414**, 153 (2017).
[35] T. Matsushima, J. Phys. Chem. C **111**, 6422 (2007).
[36] K. Imamura and T. Matsushima, Catal. Lett. **97**, 197 (2004).
[37] I. Kobal, A. Kokalj, H. Horino, Y. Ohno, and T. Matsushima, Trends Chem. Phys. **10**, 139 (2002).
[38] S. Haq and A. Hodgson, Surf. Sci. **463**, 1 (2000).
[39] H. H. Huang, C. S. Seet, Z. Zou, and G. Q. Xu, Surf. Sci. **356**, 181 (1996).
[40] Y. Ohno, K. Kimura, M. Bi, and T. Matsushima, J. Chem. Phys. **110**, 8221 (1999).

[41] A. Hodgson, Prog. Surf. Sci. **63**, 1 (2000).
[42] M. J. Cardillo, M. Balooch, and R. E. Stickney, Surf. Sci. **50**, 263 (1975).
[43] C. T. Rettner, H. A. Michelsen, and D. J. Auerbach, J. Chem. Phys. **102**, 4625 (1995).
[44] T. Yamanaka and T. Matsushima, Rev. Sci. Instrum. **78**, 034105 (2007).
[45] A. Winkler, M. Kratzer, G. Pauer, C. Eibl, and D. Gleispach, Top. Catal. **46**, 189 (2007).

All articles published on e-J. Surf. Sci. Nanotechnol. are licensed under the Creative Commons Attribution 4.0 International (CC BY 4.0). You are free to copy and redistribute articles in any medium or format and also free to remix, transform, and build upon articles for any purpose (including a commercial use) as long as you give appropriate credit to the original source and provide a link to the Creative Commons (CC) license. If you modify the material, you must indicate changes in a proper way.

Copyright: ©2025 The author(s)
Published by The Japan Society of Vacuum and Surface Science